Electronic Supplementary Material (ESI) for Inorganic Chemistry Frontiers.
This journal is © the Partner Organisations 2021

*Supporting Information*

# pH manipulates the assembly of a series of dysprosium clusters with subtle differences

Hai-Ling Wang,[a] Tong Liu,[a] Zhong-Hong Zhu,[a,b,*] Jin-Mei Peng,[a] Hua-Hong Zou,[a,*] Fu-Pei Liang[a,c,*]

[a]State Key Laboratory for Chemistry and Molecular Engineering of Medicinal Resources, School of Chemistry and Pharmacy of Guangxi Normal University, Guilin 541004, P. R. China

[b]State Key Laboratory of Luminescent Materials and Devices, School of Materials Science and Engineering, South China University of Technology, 510640, Guangzhou, China

[c]Guangxi Key Laboratory of Electrochemical and Magnetochemical Functional Materials, College of Chemistry and Bioengineering, Guilin University of Technology, Guilin 541004, P. R. China

*E-mail (Corresponding author): 18317725515@163.com (Z.-H. Zhu), gxnuchem@foxmail.com (H.-H. Zou), fliangoffice@yahoo.com (F.-P. Liang).

## Table of Contents

| | |
|---|---|
| | clusters **1**–**5** (b, d, f, h and j). |
| **Figure S11** | Loop curve graph of clusters **1**–**5** at 2 K. |
| **Figure S12** | Temperature-dependent $\chi'$ and $\chi''$ AC susceptibilities under 0 DC fields for **1**–**5** (a–e); Cole–Cole plots for **1**–**5** (f–j), solid lines are the best fits to the Debye model; ln($\tau$) *vs.* $T^{-1}$ plots for **1**–**5** (k–o), solid lines show the best fits with the Debye formula (linear). |
| **Figure S13** | Temperature-dependent $\chi'$ and $\chi''$ AC susceptibilities under 1800 Oe DC fields for **1**-**5** (a–e). |

## Experimental Section

### Materials and Measurements.

All reagents were obtained from commercial sources and used without further purification. Elemental analyses for C, and H were performed on a vario MICRO cube. Infrared spectra were recorded by transmission through KBr pellets containing *ca.* 0.5% of the complexes using a PE Spectrum FT-IR spectrometer (400-4,000 $cm^{-1}$; Figure S1). Thermogravimetric analyses (TGA) were conducted in a flow of nitrogen at a heating rate of 5 °C/min using a NETZSCH TG 209 F3 (Figure S2). Powder X-ray diffraction (PXRD) spectra were recorded on either a D8 Advance (Bruker) diffractometer at 293 K (Mo-Kα). The samples were prepared by crushing crystals and the powder placed on a grooved aluminum plate. Diffraction patterns were recorded from 5º to 55º at a rate of 5º $min^{-1}$ (Figure S3). Measurements of magnetic susceptibility were carried out within the temperature range of 2–300 K using a Quantum Design MPMS SQUID magnetometer equipped with a 5 T magnet. The diamagnetic corrections for these complexes were estimated using Pascal's constants, and magnetic data were corrected for diamagnetic contributions of the sample holder. Alternating current susceptibility measurements were performed from powdered samples to determine the in-phase and out-of-phase components of the magnetic susceptibility. The data were collected by increasing the temperature from 2 K to 15 K within frequencies ranging from 1 to 1,000 Hz, under 0 Oe and 1800 Oe. In the samples where free movement of crystallites was prevented, silicone grease was employed for embedding.

### Single-crystal X-ray crystallography.

Diffraction data for the complex were collected on a Bruker SMART CCD diffractometer (Mo-Kα radiation and $\lambda$ = 0.71073 Å) in $\Phi$ and $\omega$ scan modes. The structures were solved by direct methods, followed by difference Fourier syntheses, and then refined by full-matrix least-squares techniques on $F^2$ using *SHELXL*[1]. All other non-hydrogen atoms were refined with anisotropic thermal parameters. Hydrogen atoms were placed at calculated positions and isotropically refined using a riding model. Table S1 summarizes X-ray crystallographic data and refinement details for the all complexes. The CCDC reference numbers are 2061004, 2061003, 2061002, 2060963 and 2060964 for **1**–**5**. Before this, our group has reported the synthesis and structure of cluster **4**.[2]

### The synthesis method.

**$H_4L^1$–$H_4L^2$**: The synthesis of organic ligands $H_4L^1$–$H_4L^2$ refers to the reported method.[3]

**1**: Add 0.05 mmol (approximately 25 mg) ligand $H_4L^1$, 0.4 mmol $Dy(OAc)_3·6H_2O$ (approximately 180 mg), 1.5 mL $CH_3OH$, 0.5 mL $CH_3CN$, and 0.15 mL HOAc to the Pyrex whose one end is about 25 cm long. The pH value of the mixed system was about 6.4. In the tube, shake and sonicate for 15 min. Place the sealed Pyrex tube in an oven at 80 ˚C, take it out three days later, slowly cool to room temperature, and precipitate yellow lumpy crystals. The yield is about 38.3% (Scheme S1 and S2, calculated with the amount of ligand). Elemental analysis theoretical value ($C_{66}H_{57}Dy_5N_{12}O_{23}$): C, 37.41%; H, 2.88%; N, 7.27%; experimental value: C, 37.18%; H, 2.62%; N, 7.51%. Infrared spectrum data (IR, KBr pellet, $cm^{-1}$): 3428.81(m), 2354.89(w), 1361.52(m), 1192.87(m), 898.77(m), 717.79(w).

**2**: Add 0.05 mmol (approximately 25 mg) ligand $H_4L^1$, 0.4 mmol $Dy(OAc)_3·6H_2O$ (approximately 180 mg), 1.5 mL $CH_3OH$, 0.5 mL $CH_3CN$, and 0.17 mL HOAc to the Pyrex whose one end is about 25 cm long. The pH value of the mixed system was about 6.6. In the tube, shake and sonicate for 15 min. Place the sealed Pyrex tube in an oven at 80 ˚C, take it out three days later, slowly cool to room temperature, and precipitate brown lumpy crystals. The yield is about 55.3% (calculated with the amount of ligand). Elemental analysis theoretical value ($C_{67}H_{61}Dy_5N_{12}O_{25}$): C, 35.82%; H, 2.74%; N, 7.48%; experimental value: C, 35.51%; H, 3.08%; N, 7.21%. Infrared spectrum data (IR, KBr pellet, $cm^{-1}$): 3411(m), 2344.61(w), 1380(m), 1208(m), 863.80( m), 5524.45(w).

**3**: Add 0.05 mmol (approximately 25 mg) ligand $H_4L^1$, 0.4 mmol $Dy(OAc)_3·6H_2O$ (approximately 180 mg), 1.5 mL $CH_3OH$, 0.5 mL $CH_3CN$, and 0.15 mL triethylamine to the Pyrex whose one end is about 25 cm long. The pH value of the mixed system was about 9.0. In the tube, shake and sonicate for 15 min. Place the sealed Pyrex tube in an oven at 80 ˚C, take it out three days later, slowly cool to room temperature, and precipitate yellow lumpy crystals. The yield is about 58.4% (calculated with the amount of ligand). Elementary analysis theoretical value ($C_{72}H_{66}Dy_5N_{12}O_{25}$): C, 37.14%; H, 2.88%; N, 7.27%; experimental value: C, 37.18%; H, 2.62%; N, 7.51%. Infrared spectrum data (IR, KBr pellet, $cm^{-1}$): 3442.32(m), 2341.59(w), 1338.89(m), 1203.15(m), 660.19(m), 536.79(w).

**4**: Before this, our group has reported the synthesis and structure of cluster **4**.[2] Add 0.05 mmol (approximately 27 mg) ligand $H_4L^2$, 0.4 mmol $Dy(OAc)_3·6H_2O$ (approximately 180 mg), 1.5 mL $CH_3OH$, 0.5 mL $CH_3CN$, and 0.15 mL HOAc to the Pyrex whose one end is about 25 cm long. The pH value of the mixed system was about 6.8. In the tube, shake and sonicate for 15 min. Place the sealed Pyrex tube in an oven at 80 ˚C, take it out three days later, slowly cool to room temperature,

and precipitate yellow lumpy crystals. The yield is about 52.1% (calculated with the amount of ligand). Elementary analysis theoretical value ($C_{76}H_{87}Dy_5N_{12}O_{29}$): C, 37.33%; H, 3.59%; N, 6.87%; experimental value: C, 37.11%; H, 3.81%; N, 6.51%. Infrared spectrum data (IR, KBr pellet, $cm^{-1}$): 3427.47(m), 2345.68(w), 1344.71(m), 116.08(m), 865.54(m), 751.89(w).

**5**: Add 0.05 mmol (approximately 27 mg) ligand $H_4L^2$, 0.4 mmol $Dy(OAc)_3 \cdot 6H_2O$ (approximately 180 mg), 1.5 mL $CH_3OH$, 0.5 mL $CH_3CN$, and 0.15 mL triethylamine to the Pyrex whose one end is about 25 cm long. The pH value of the mixed system was about 9.2. In the tube, shake and sonicate for 15 min. Place the sealed Pyrex tube in an oven at 80 ˚C, take it out three days later, slowly cool to room temperature, and precipitate yellow lumpy crystals. The yield is about 50.6% (calculated with the amount of ligand). Elementary analysis theoretical value ($C_{81}H_{80}Dy_6N_{12}O_{31}$): C, 36.13%; H, 2.99%; N, 6.24%; experimental value: C, 35.82%; H, 3.14%; N, 6.02%. Infrared spectrum data (IR, KBr pellet, $cm^{-1}$): 3430.24(m), 2373.34(w), 1342.80(m), 1166.19(m), 865.01(m), 751.24(w).

**Table S1.** Crystallographic data of the clusters **1**–**5**.

| | **1** | **2** | **3** | **4** | **5** |
|---|---|---|---|---|---|
| Formula | $C_{66}H_{57}Dy_5N_{12}O_{23}$ | $C_{67}H_{61}Dy_5N_{12}O_{25}$ | $C_{72}H_{66}Dy_5N_{12}O_{25}$ | $C_{76}H_{84}Dy_5N_{12}O_{29}$ | $C_{81}H_{80}Dy_6N_{12}O_{31}$ |
| Formula weight | 2198.73 | 2246.77 | 2311.86 | 2442.05 | 2692.57 |
| $T$, K | 293(2) | 293(2) | 293(2) | 100.00(10) | 100.00(10) |
| Crystal system | triclinic | triclinic | triclinic | triclinic | monoclinic |
| Space group | *P*-1 | *P*-1 | *P*-1 | *P*-1 | *C*2/*c* |
| $a$, Å | 15.6215(3) | 15.4027(2) | 15.3856(2) | 13.7272(3) | 20.8164(5) |
| $b$, Å | 16.9622(3) | 15.9505(3) | 16.2878(2) | 16.0947(4) | 17.9779(3) |
| $c$, Å | 20.0435(4) | 19.8366(4) | 19.7277(2) | 22.9040(4) | 24.0351(6) |
| $\alpha$, ° | 74.828(2) | 108.286(2) | 78.4020(10) | 103.687(2) | 90 |
| $\beta$, ° | 73.689(2) | 95.0240(10) | 74.5510(10) | 91.817(2) | 110.414(3) |
| $\gamma$, ° | 62.780(2) | 102.3810(10) | 78.4430(10) | 114.999(2) | 90 |
| $V$, Å$^3$ | 4477.19(17) | 4456.31(15) | 4611.04(10) | 4405.87(18) | 8429.9(4) |
| $Z$ | 2 | 2 | 2 | 2 | 4 |
| $D_c$, g cm$^{-3}$ | 1.631 | 1.674 | 1.665 | 1.828 | 2.122 |
| $\mu$, mm$^{-1}$ | 4.189 | 22.630 | 21.891 | 4.272 | 5.344 |
| $F$(000) | 2102.0 | 2154.0 | 2224.0 | 2355.0 | 5175.0 |
| 2$\theta$ range for data collection/° | 3.332,60.456 | 4.8, 153.2 | 4.7, 153.3 | 3.7,62.0 | 3.9,51.0 |
| Tot. Data | 51813 | 54969 | 57142 | 67053 | 31714 |
| Uniq. Data | 20688 | 18000 | 18701 | 22306 | 7848 |
| $R_{int}$ | 0.0428 | 0.051 | 0.046 | 0.0557 | 0.0325 |
| Observed | | | | | |

| | | | | | |
|---|---|---|---|---|---|
| data [$I >$ $2\sigma(I)$] | 20688 | | | 22306 | 7848 |
| $N_{ref}$, $N_{par}$ | 16,976 | 18, 1007 | 11, 1051 | 6,1131 | 1298,691 |
| $R_1$[a] ($I >$ $2\sigma(I)$) | 0.0468 | 0.0481 | 0.0432 | 0.0517 | 0.0424 |
| $wR_2$[b] (all data) | 0.1319 | 0.1448 | 0.1335 | 0.1280 | 0.1097 |
| GOF | 1.022 | 1.108 | 1.130 | 1.010 | 1.052 |

[a]$R_1 = \Sigma||F_o|-|F_c||/\Sigma|F_o|$, [b]$wR_2 = [\Sigma w(F_o^2-F_c^2)^2/\Sigma w(F_o^2)^2]^{1/2}$

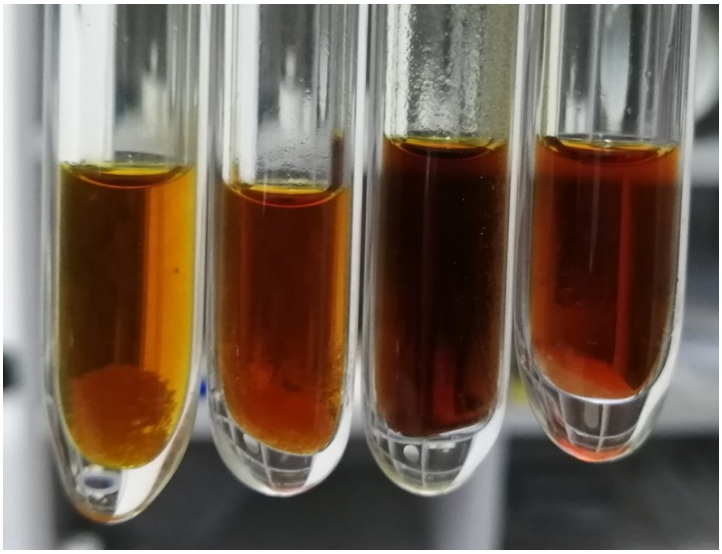

**Scheme S1.** The cluster **1** crystals obtained after the reaction.

a)

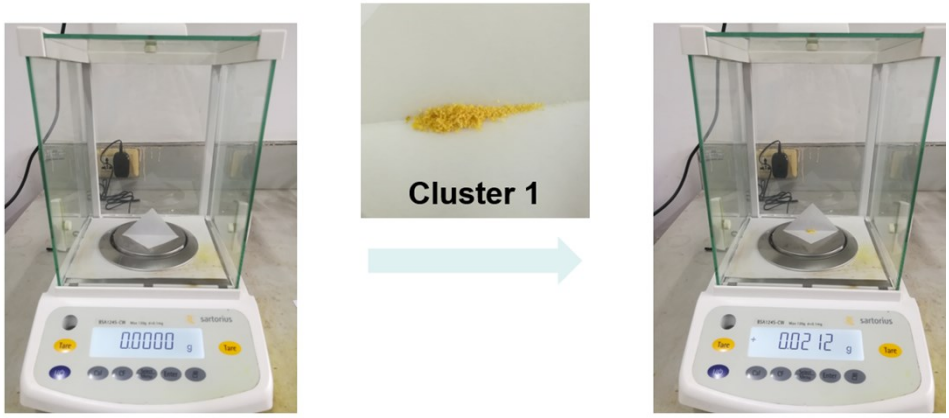


b) $m_{theoretical} = 0.025 \times 2198.73 = 54.96$ mg

$m_{experimental} = 21.20$ mg

Yield = $m_{experimental} / m_{theoretical} \times 100\ \% = 38.6\ \%$

**Scheme S2.** The yield of cluster **1** obtained.

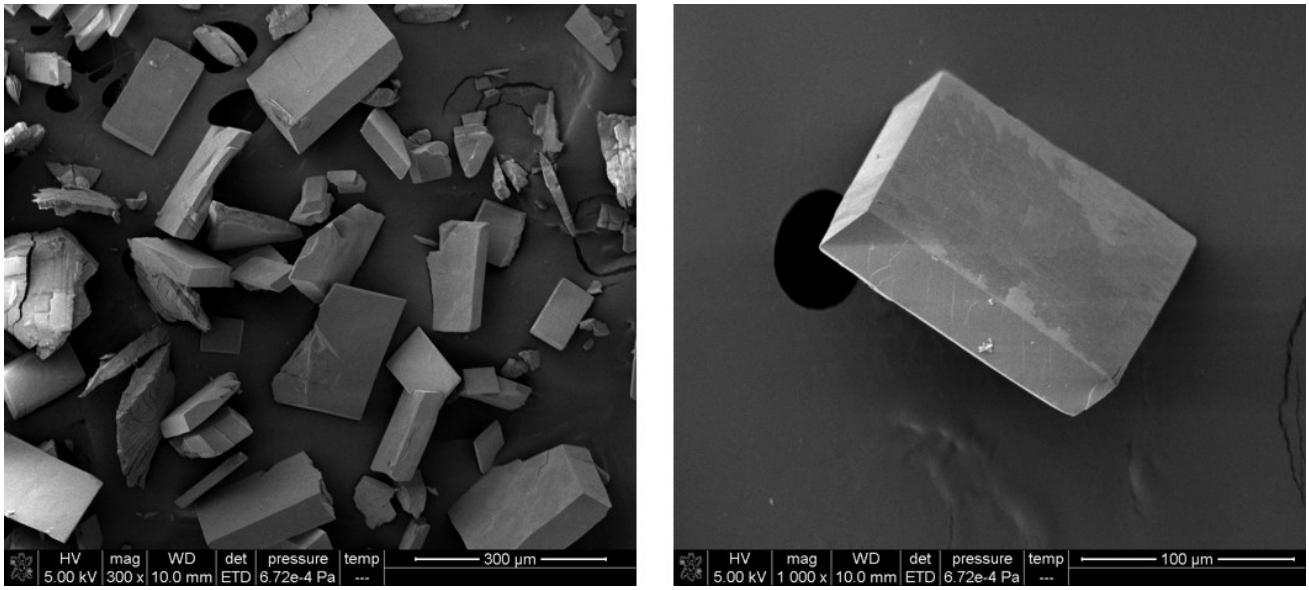


**Scheme S3.** SEM picture of cluster **1** crystals.

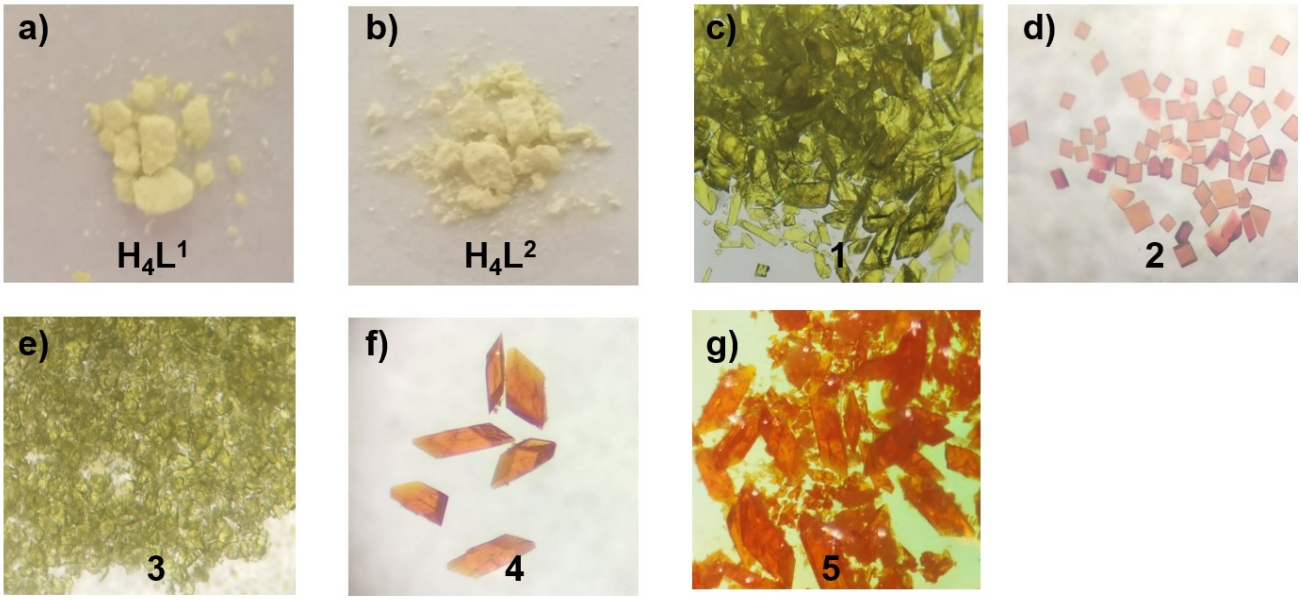


**Scheme S4.** Photographs of ligand powder (a and b) and crystals **1**-**5** (c-g).

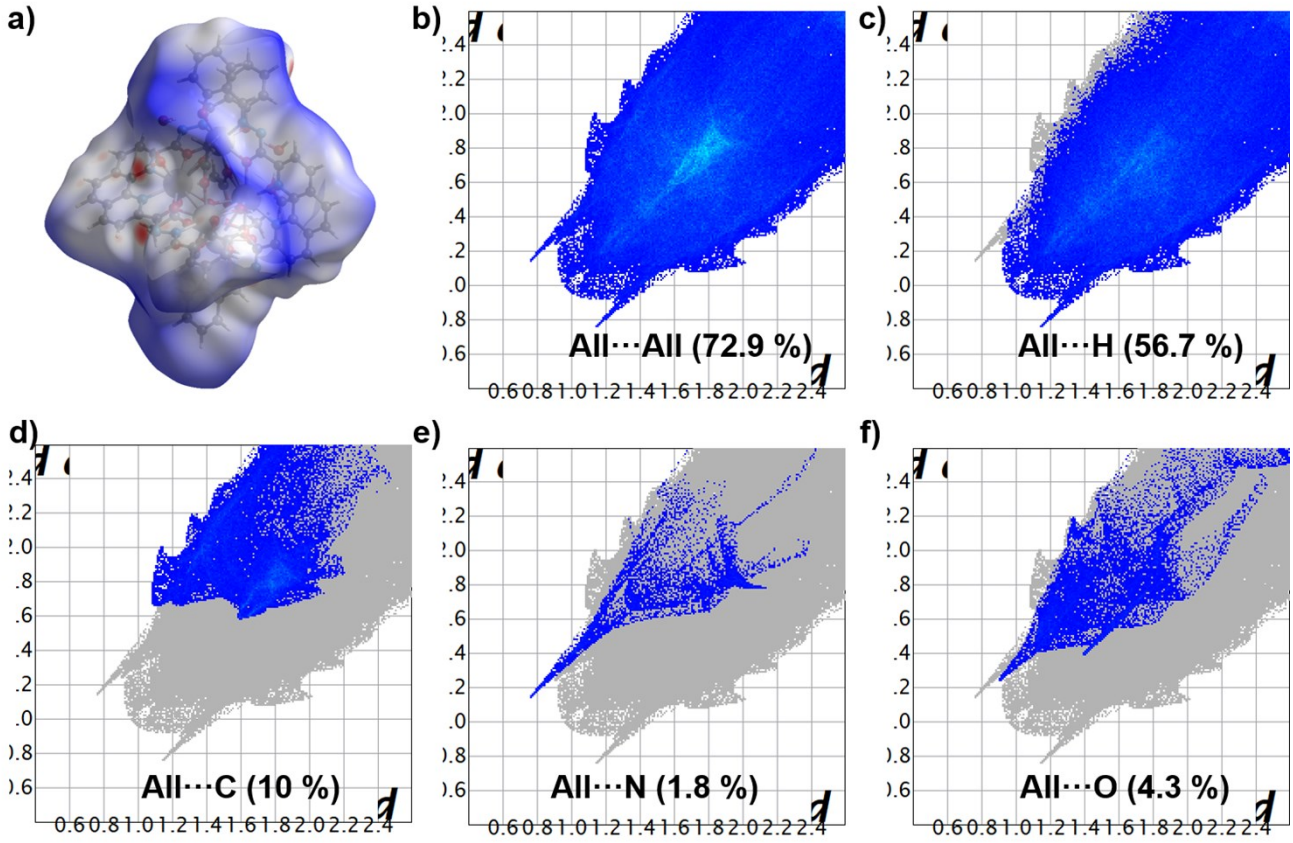


**Figure S1.** Hirshfeld surfaces mapped with $d_{norm}$ (a) and 2D fingerprint plots (b-f) for the cluster **1**.

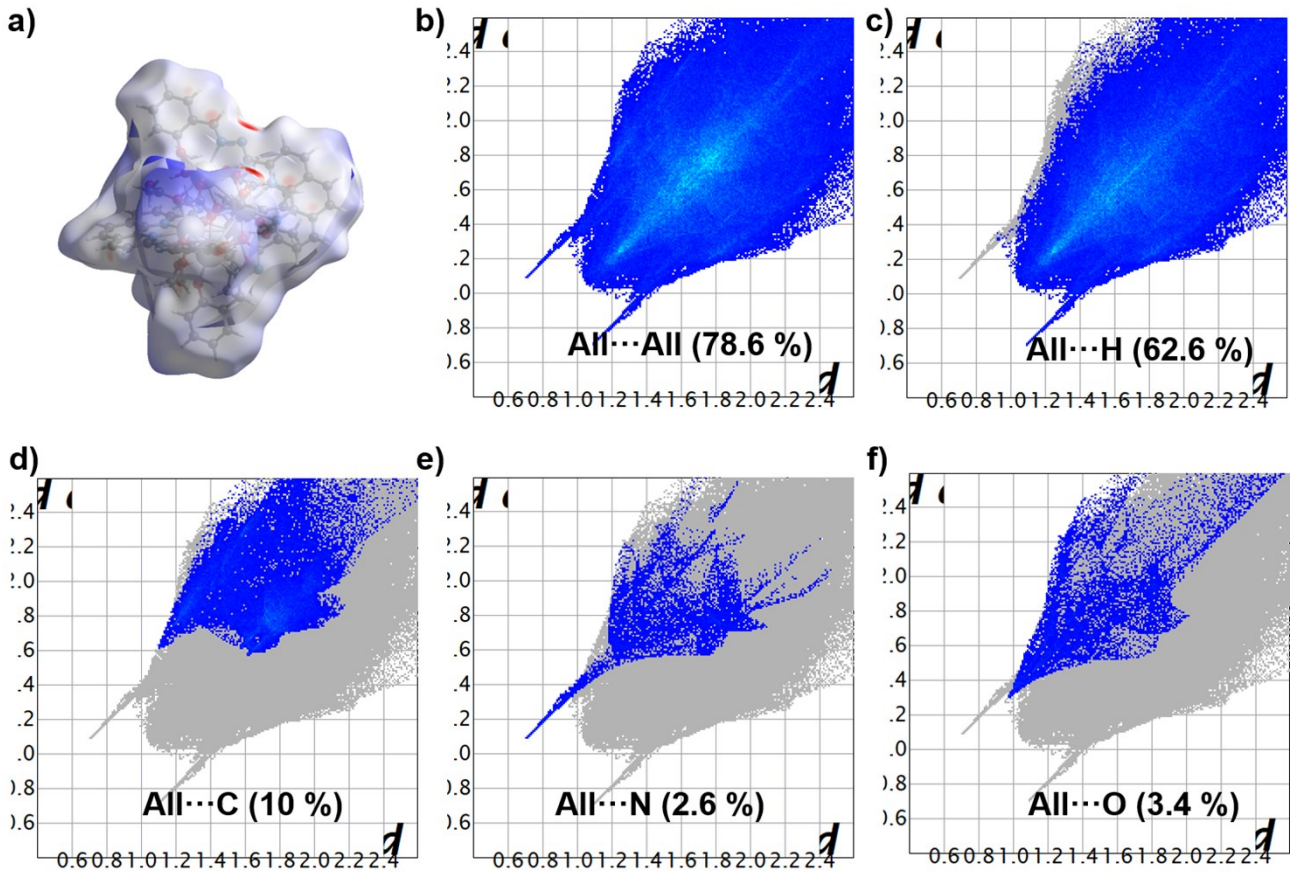


**Figure S2.** Hirshfeld surfaces mapped with $d_{norm}$ (a) and 2D fingerprint plots (b-f) for the cluster **2**.

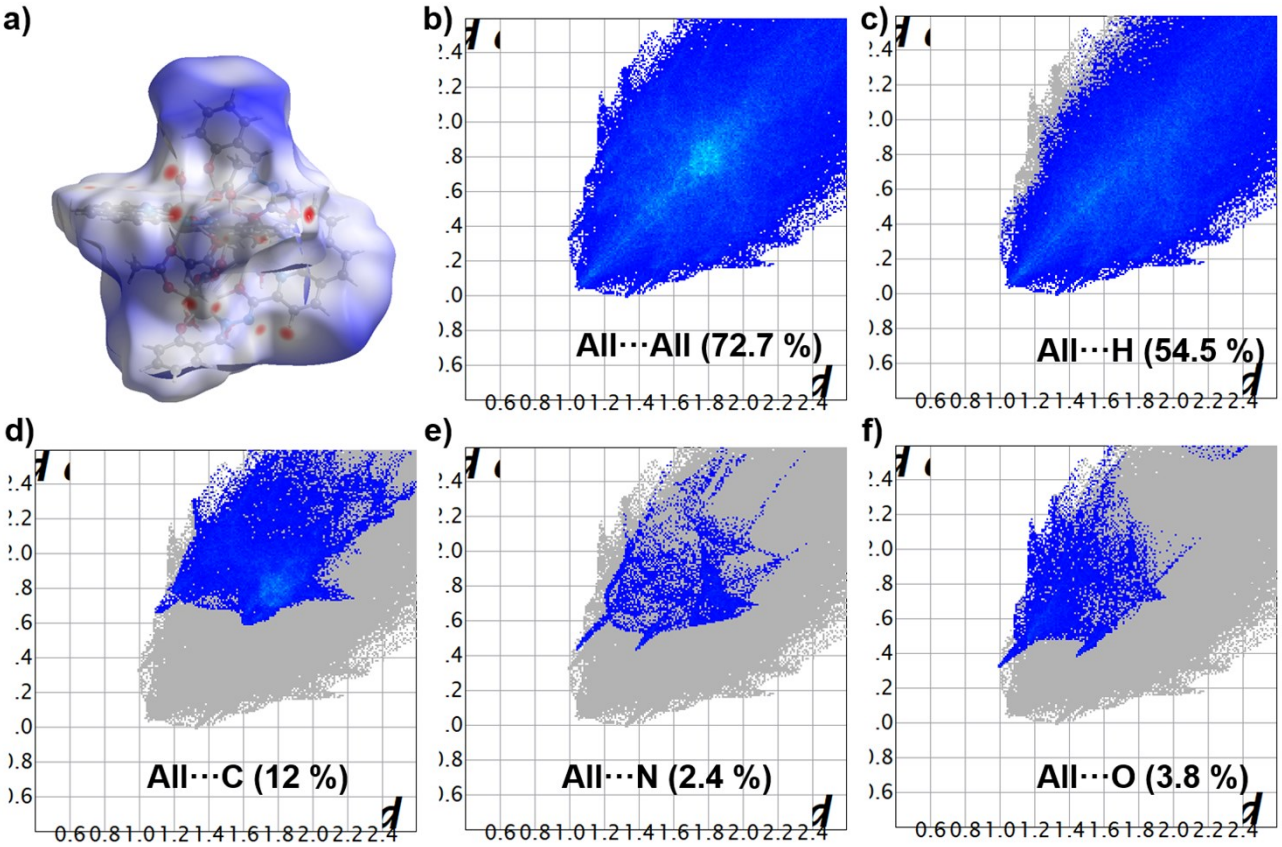


**Figure S3.** Hirshfeld surfaces mapped with $d_{norm}$ (a) and 2D fingerprint plots (b-f) for the cluster **3**.

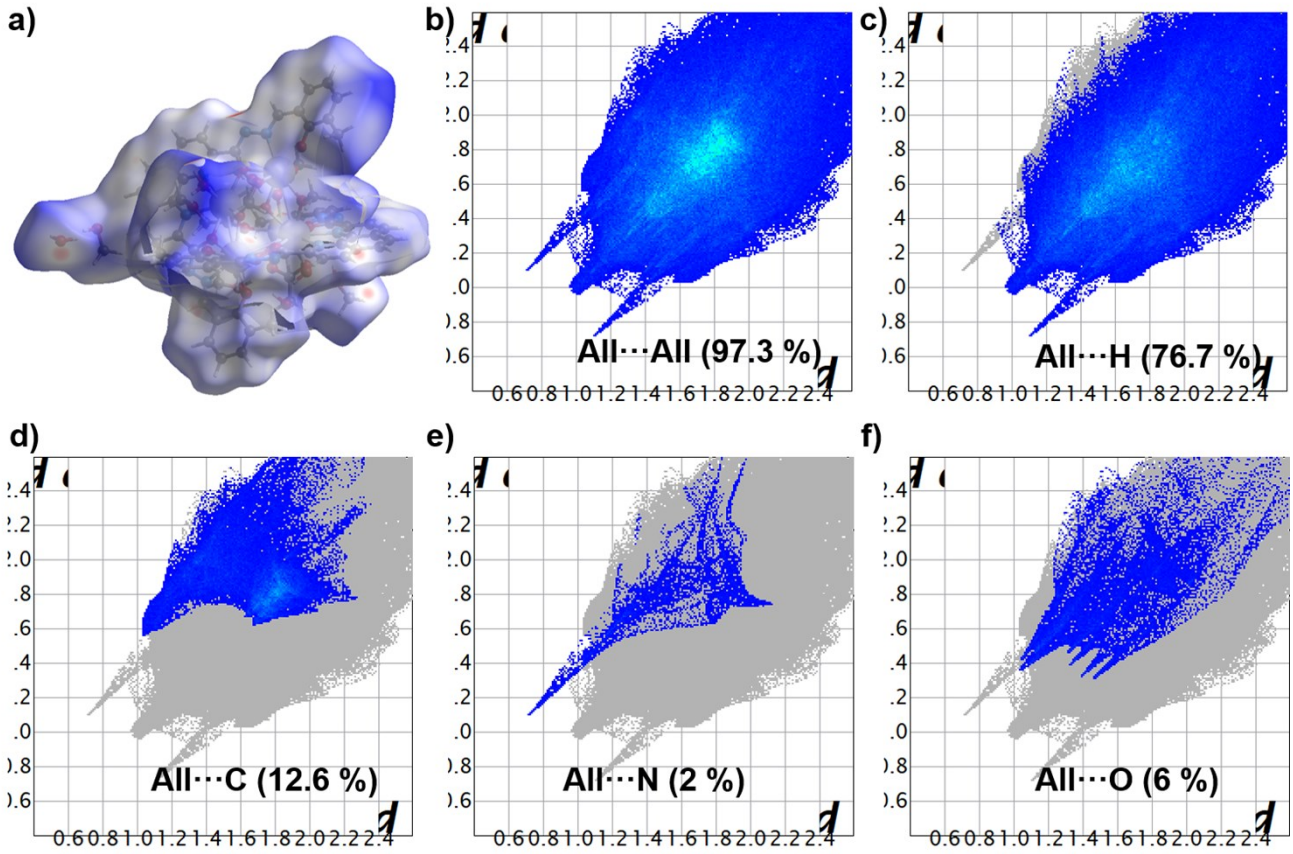


**Figure S4.** Hirshfeld surfaces mapped with $d_{norm}$ (a) and 2D fingerprint plots (b-f) for the cluster **4**.

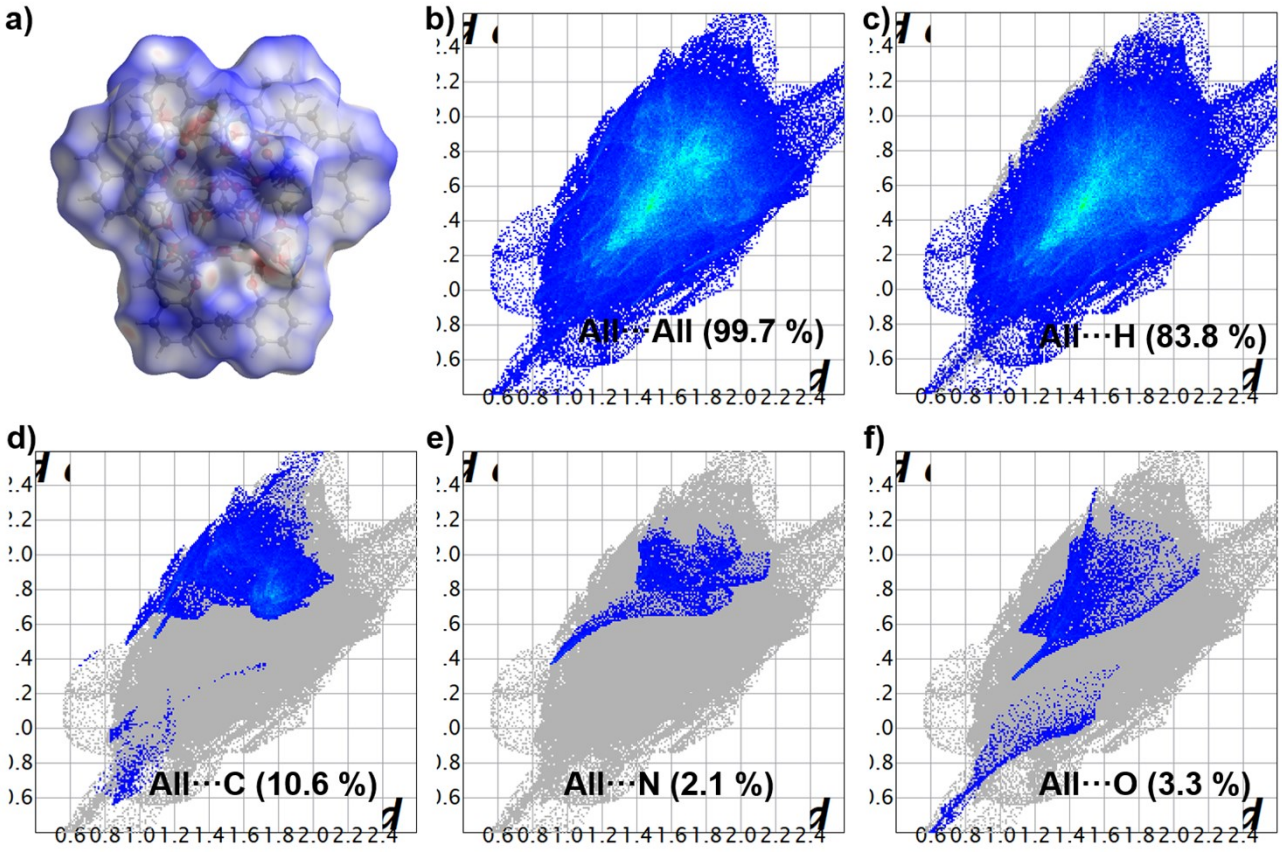


**Figure S5.** Hirshfeld surfaces mapped with $d_{norm}$ (a) and 2D fingerprint plots (b-f) for the cluster **5**.

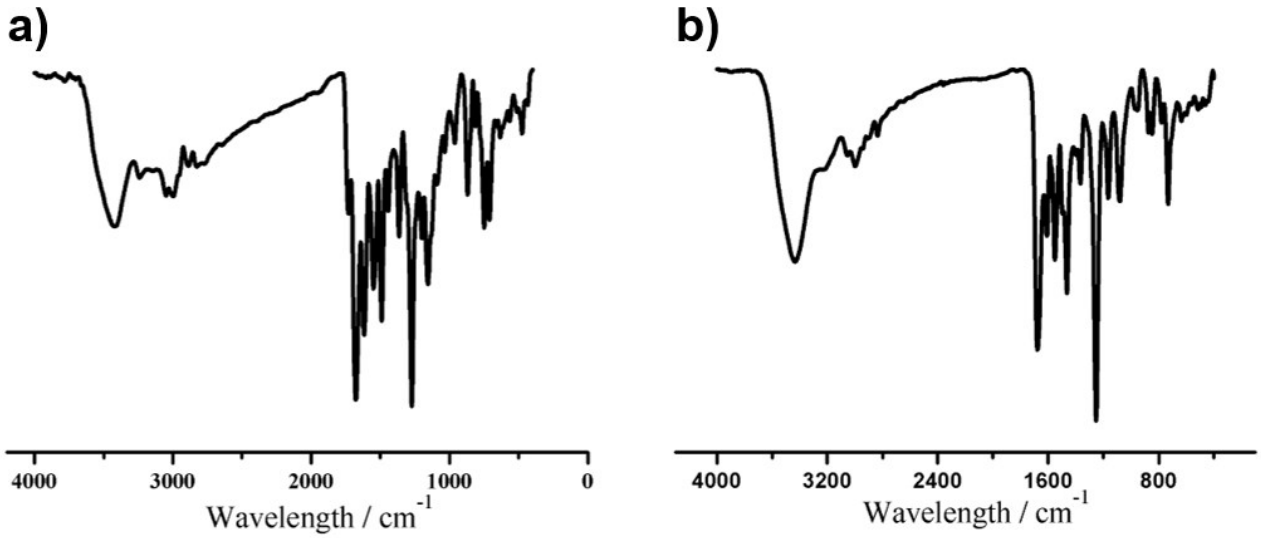


**Figure S6.** Infrared spectra (IR) of ligands $H_4L^1$ (a) and $H_4L^2$ (b).

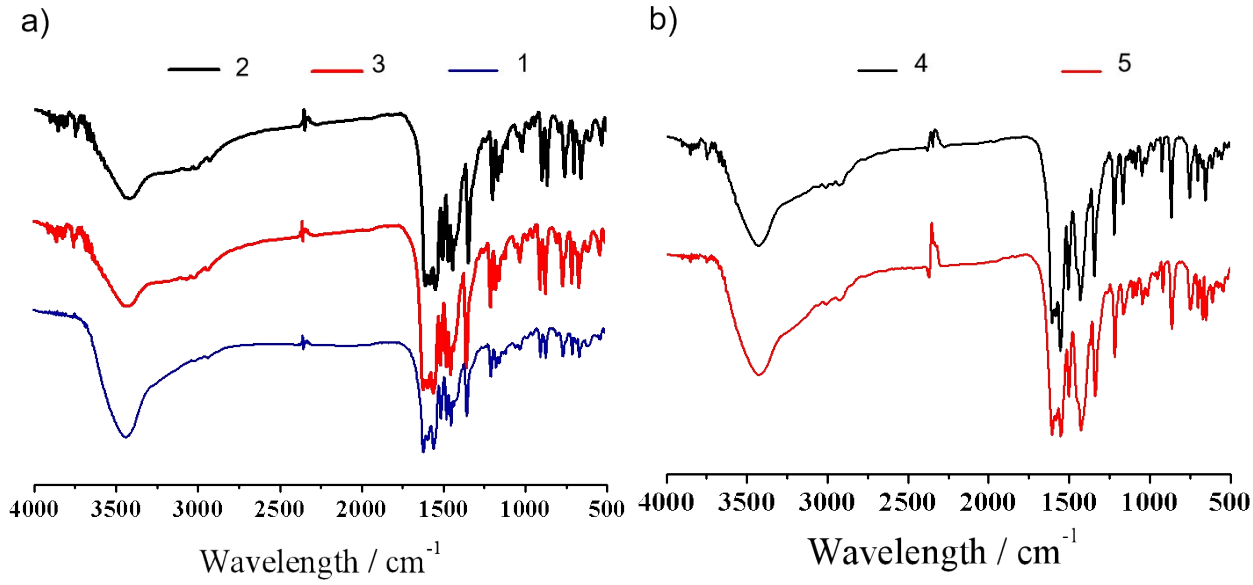


**Figure S7.** Infrared spectra (IR) of clusters **1**–**3** (a) and **4**–**5** (b).

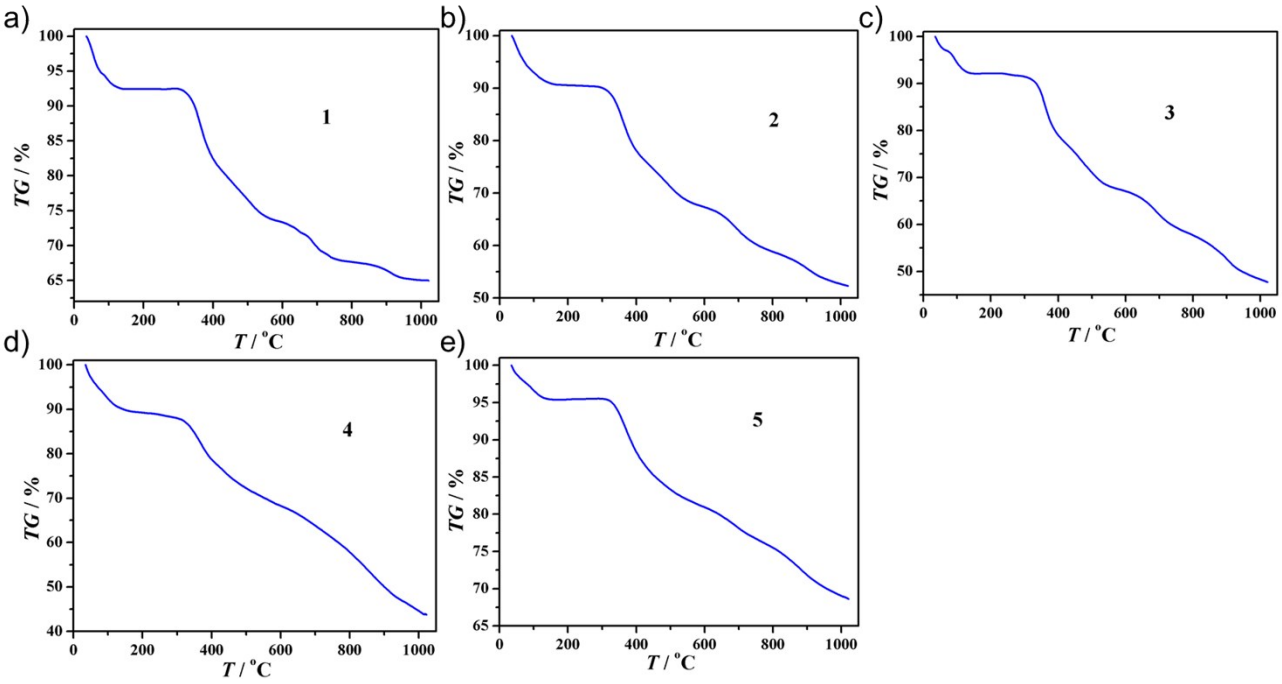


**Figure S8.** TG curves of clusters **1-5** (a–e).

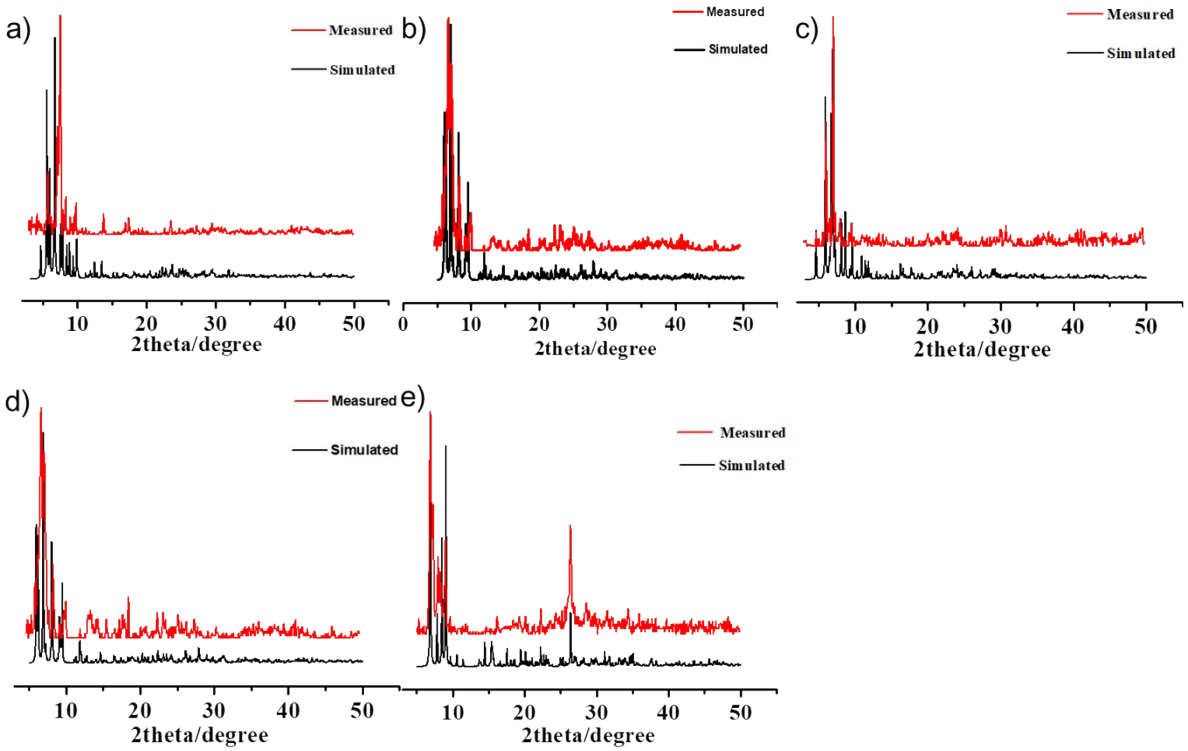


**Figure S9.** Powder diffraction pattern (PXRD) of clusters **1**–**5** (a–e).

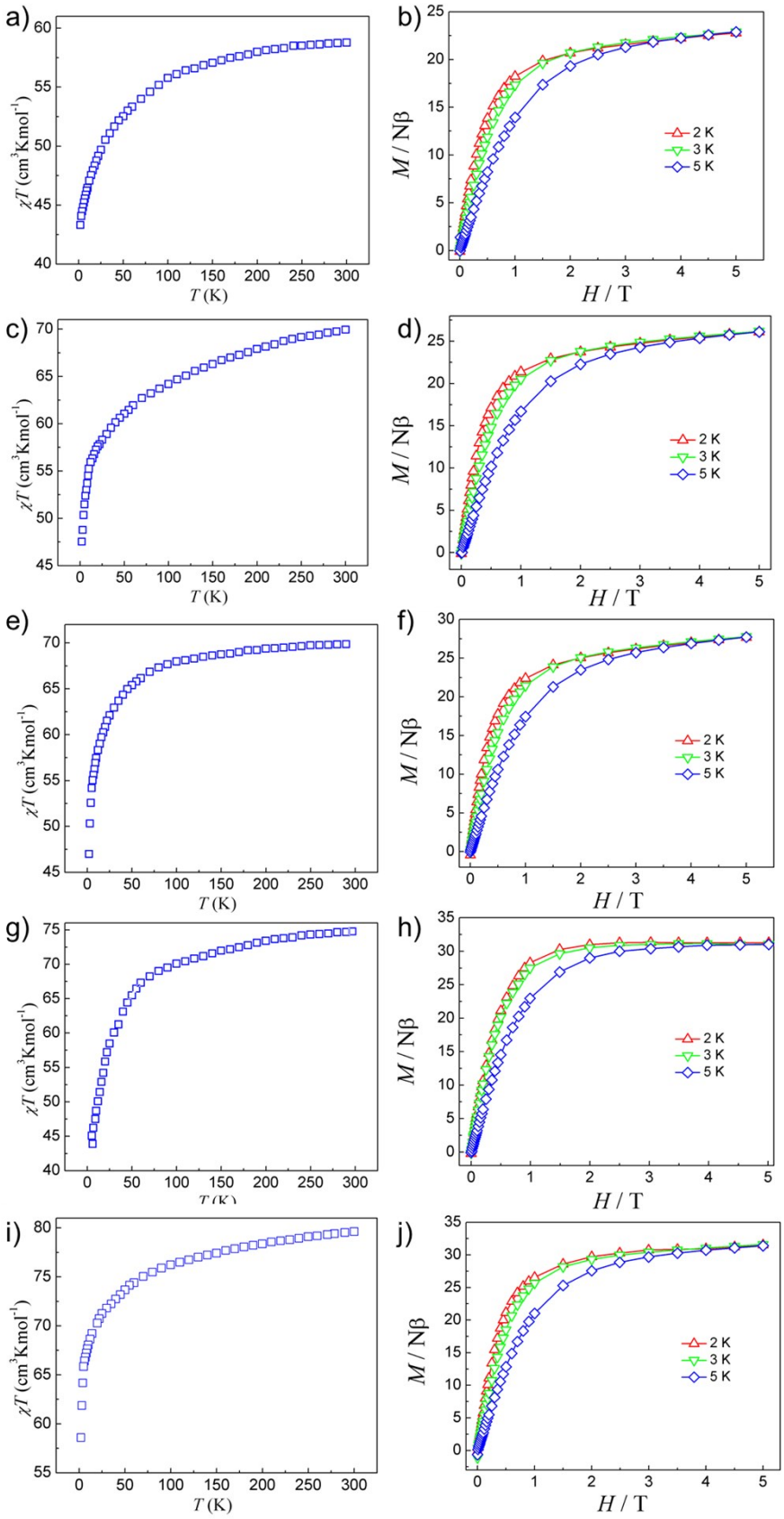


**Figure S10.** Temperature dependence of $\chi_m T$ for clusters **1**–**5** (a, c, e, g, and i); $M$ vs. $H$ plots of clusters **1**–**5** (b, d, f, h and j).

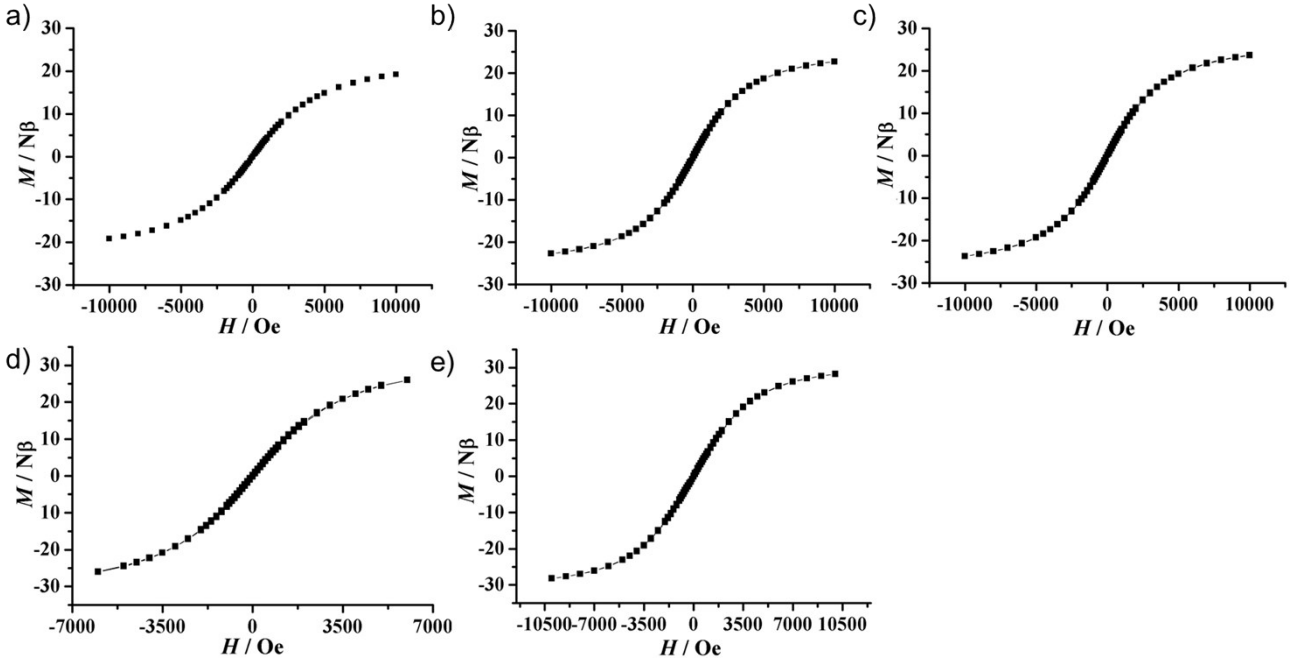


**Figure S11.** Loop curve graph of clusters **1**–**5** (a–e) at 2 K.

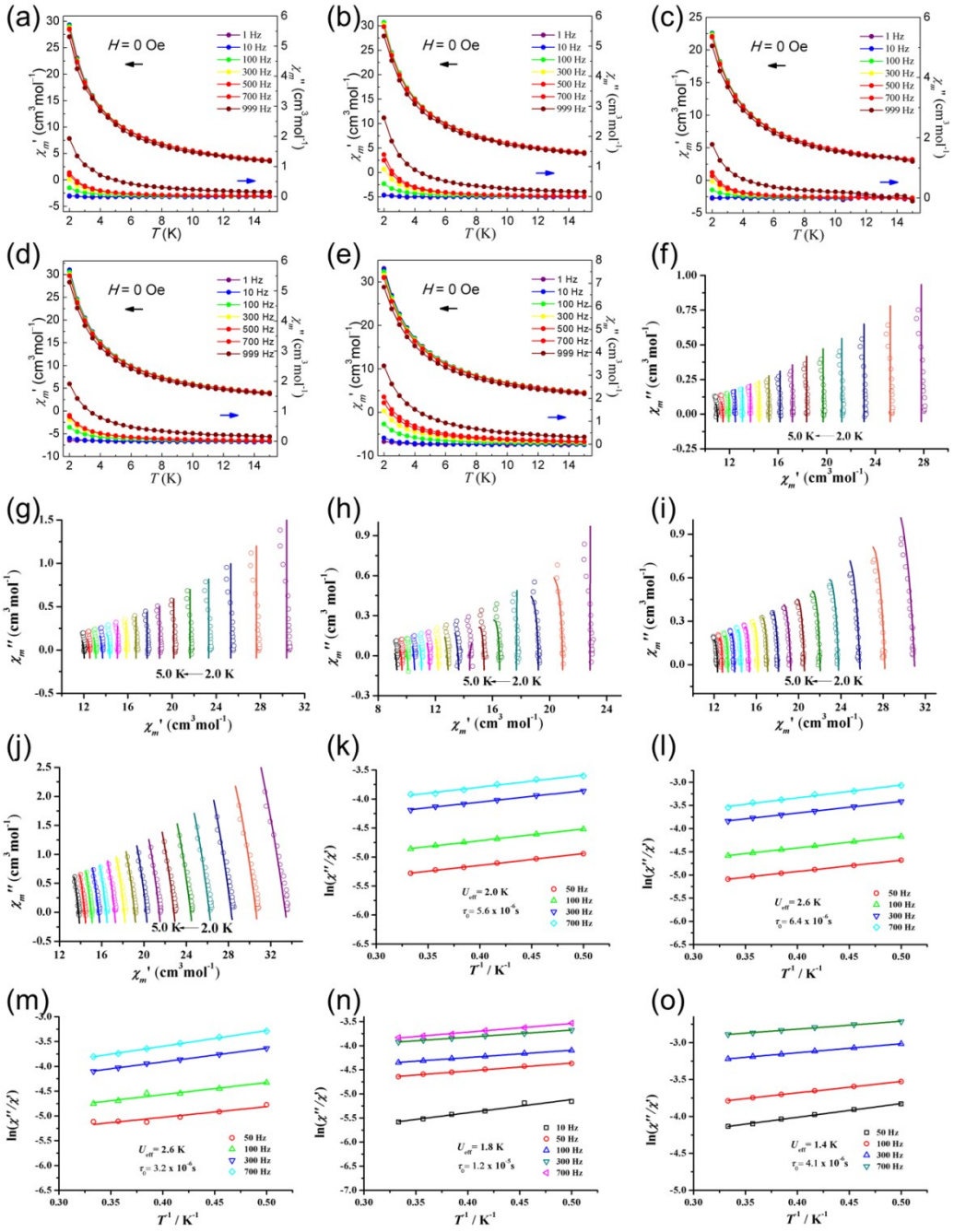


**Figure S12.** Temperature-dependent $\chi'$ and $\chi''$ AC susceptibilities under 0 DC fields for **1**–**5** (a–e); Cole–Cole plots for **1**–**5** (f–j), solid lines are the best fits to the Debye model; ln($\tau$) *vs.* $T^{-1}$ plots for **1**–**5** (k–o), solid lines show the best fits with the Debye formula (linear).

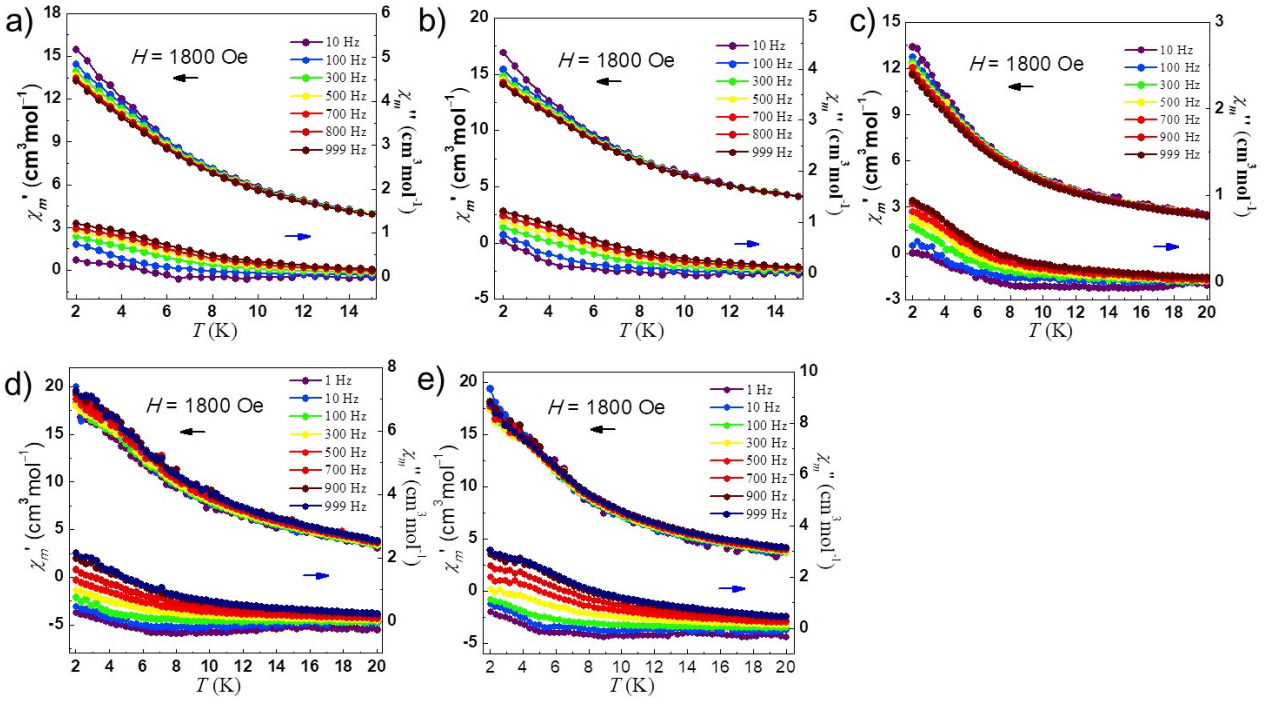


**Figure S13.** Temperature-dependent $\chi$' and $\chi$'' AC susceptibilities under 1800 Oe DC fields for **1**–**5** (a–e).

**Table S2.** Selected bond lengths (Å) and angles (°) of **1**.

| Bond lengths (Å) | | | | | |
|---|---|---|---|---|---|
| Dy1-O12 | 2.310(6) | Dy2-O20 | 2.391(4) | Dy4-O20 | 2.373(4) |
| Dy1-O16 | 2.360(5) | Dy2-O19 | 2.241(5) | Dy4-O3 | 2.312(4) |
| Dy1-O14 | 2.372(5) | Dy2-O13 | 2.597(5) | Dy4-O2 | 2.332(4) |
| Dy1-O8 | 2.221(5) | Dy3-O3 | 2.354(5) | Dy4-O21 | 2.368(5) |
| Dy1-O7 | 2.407(5) | Dy3-O4 | 2.207(5) | Dy4-O15 | 2.250(5) |
| Dy1-O22 | 2.384(7) | Dy3-O13 | 2.406(5) | Dy5-O20 | 2.387(4) |
| Dy1-O23 | 2.418(6) | Dy3-O6 | 2.391(5) | Dy5-O19 | 2.224(4) |
| Dy1-N12 | 2.478(6) | Dy3-O10 | 2.462(4) | Dy5-O1 | 2.224(4) |
| Dy2-O20 | 2.391(4) | Dy3-O5 | 2.249(6) | Dy5-O2 | 2.316(4) |
| Dy2-O19 | 2.241(5) | Dy3-N7 | 2.486(7) | Dy5-O9 | 2.322(5) |
| Dy2-O13 | 2.597(5) | Dy3-N6 | 2.509(6) | Dy5-O11 | 2.276(5) |
| Dy2-O17 | 2.368(6) | Dy4-O20 | 2.373(4) | Dy5-N1 | 2.536(5) |

| | | | | | |
|---|---|---|---|---|---|
| Dy2-O14 | 2.659(5) | Dy4-O3 | 2.312(4) | | |
| Dy2-O6 | 2.430(5) | Dy4-O2 | 2.332(4) | | |
| **Bond angles (°)** | | | | | |
| O8-Dy1-O12 | 91.1(2) | O6-Dy2-O13 | 61.27(16) | O20-Dy4-N3 | 122.91(17) |
| O8-Dy1-O16 | 80.2(2) | O6-Dy2-O14 | 110.11(16) | O20-Dy4-N4 | 150.62(18) |
| O8-Dy1-O14 | 158.31(18) | O6-Dy2-N10 | 124.42(17) | O3-Dy4-O20 | 105.03(16) |
| O8-Dy1-O7 | 136.83(18) | O3-Dy3-O13 | 75.87(17) | O3-Dy4-O2 | 165.88(17) |
| O8-Dy1-O22 | 100.7(3) | O3-Dy3-O6 | 121.44(15) | O3-Dy4-O21 | 92.32(17) |
| O8-Dy1-O23 | 82.6(2) | O3-Dy3-O10 | 64.80(15) | O3-Dy4-O10 | 65.50(16) |
| O8-Dy1-N12 | 72.80(19) | O3-Dy3-N7 | 142.3(2) | O19-Dy5-O20 | 70.87(16) |
| O7-Dy1-O23 | 126.8(2) | O3-Dy3-N6 | 63.41(18) | O19-Dy5-O1 | 87.50(17) |
| O6-Dy2-O13 | 61.27(16) | O4-Dy3-O3 | 133.36(19) | O19-Dy5-O2 | 139.74(17) |
| O6-Dy2-O14 | 110.11(16) | O4-Dy3-O13 | 86.48(19) | O19-Dy5-O9 | 87.14(18) |
| O6-Dy2-N10 | 124.42(17) | O4-Dy3-O6 | 86.63(18) | O19-Dy5-O11 | 95.40(19) |
| O6-Dy2-N9 | 62.88(17) | O20-Dy4-N3 | 122.91(17) | O19-Dy5-N1 | 156.91(17) |
| O7-Dy2-O13 | 109.21(16) | O20-Dy4-N4 | 150.62(18) | O1-Dy5-O20 | 158.36(16) |

**Table S3.** Selected bond lengths (Å) and angles (°) of **2**.

| **Bond lengths (Å)** | | | | | |
|---|---|---|---|---|---|
| Dy1-O2 | 2.408(5) | Dy2-O2 | 2.444(5) | Dy4-O7 | 2.310(5) |
| Dy1-O1 | 2.198(5) | Dy2-O21 | 2.388(5) | Dy4-O6 | 2.335(5) |
| Dy1-O13 | 2.361(4) | Dy2-O3 | 2.438(5) | Dy4-O21 | 2.409(4) |
| Dy1-O15 | 2.331(5) | Dy3-O6 | 2.363(5) | Dy4-O22 | 2.368(5) |
| Dy1-O11 | 2.459(5) | Dy3-O3 | 2.383(4) | Dy4-O16 | 2.249(5) |
| Dy1-O9 | 2.291(5) | Dy3-O14 | 2.351(4) | Dy5-O7 | 2.353(5) |
| Dy1-O12 | 2.482(5) | Dy3-O17 | 2.409(5) | Dy5-O21 | 2.404(4) |
| Dy1-N1 | 2.450(6) | Dy3-O5 | 2.244(5) | Dy5-O8 | 2.234(5) |
| Dy2-O2 | 2.444(5) | Dy3-O4 | 2.236(5) | Dy5-O20 | 2.271(5) |
| Dy2-O21 | 2.388(5) | Dy3-N6 | 2.484(6) | Dy5-O18 | 2.370(5) |
| Dy2-O3 | 2.438(5) | Dy3-N7 | 2.507(6) | Dy5-O10 | 2.367(6) |

| | | | | | |
|---|---|---|---|---|---|
| Dy2-O20 | 2.244(5) | Dy4-O7 | 2.310(5) | Dy5-N12 | 2.523(6) |
| Dy2-O13 | 2.647(5) | Dy4-O6 | 2.335(5) | Dy5-O23 | 2.454(7) |
| Dy2-O14 | 2.578(5) | Dy4-O21 | 2.409(4) | | |
| **Bond angles (°)** | | | | | |
| O2-Dy1-O11 | 79.49(17) | O2-Dy2-O13 | 59.37(14) | O7-Dy4-O6 | 164.56(17) |
| O2-Dy1-O12 | 117.96(17) | O6-Dy3-N7 | 62.98(17) | O7-Dy4-O21 | 70.74(16) |
| O2-Dy1-N1 | 65.14(17) | O3-Dy3-O17 | 73.43(16) | O8-Dy5-O7 | 120.63(19) |
| O2-Dy1-C60 | 98.71(17) | O3-Dy3-N6 | 64.95(18) | O8-Dy5-O21 | 153.48(19) |
| O1-Dy1-O2 | 137.86(17) | O3-Dy3-N7 | 151.58(18) | O8-Dy5-O20 | 90.59(19) |
| O1-Dy1-O13 | 157.84(18) | O14-Dy3-O6 | 75.16(17) | O8-Dy5-O18 | 82.2(2) |
| O1-Dy1-O15 | 81.31(18) | O14-Dy3-O3 | 65.32(16) | O8-Dy5-O10 | 124.1(2) |
| O2-Dy2-O13 | 59.37(14) | O14-Dy3-O17 | 87.41(17) | O8-Dy5-N12 | 70.97(19) |
| O2-Dy2-O14 | 108.63(15) | O7-Dy4-O6 | 164.56(17) | O8-Dy5-O23 | 73.3(3) |
| O2-Dy2-N3 | 62.34(16) | O7-Dy4-O21 | 70.74(16) | O20-Dy5-O7 | 134.69(17) |
| O2-Dy2-N4 | 124.00(17) | O7-Dy4-O22 | 84.14(17) | O18-Dy5-O21 | 78.15(16) |
| O2-Dy2-C62 | 83.98(16) | O7-Dy4-O17 | 98.22(17) | O20-Dy5-O7 | 134.69(17) |
| O21-Dy2-O2 | 84.58(15) | O7-Dy4-N9 | 126.91(18) | O20-Dy5-O21 | 68.80(16) |

**Table S4.** Selected bond lengths (Å) and angles (°) of **3**.

| | | | | | |
|---|---|---|---|---|---|
| **Bond lengths (Å)** | | | | | |
| Dy1-O8 | 2.197(5) | Dy2-O25 | 2.386(4) | Dy4-O2 | 2.314(4) |
| Dy1-O7 | 2.414(4) | Dy2-O6 | 2.392(4) | Dy4-O12 | 2.410(4) |
| Dy1-O15 | 2.350(4) | Dy2-O7 | 2.426(4) | Dy4-O25 | 2.429(4) |
| Dy1-O18 | 2.429(5) | Dy3-O12 | 2.481(4) | Dy4-O3 | 2.302(4) |
| Dy1-O17 | 2.450(5) | Dy3-O6 | 2.400(4) | Dy4-O14 | 2.258(4) |
| Dy1-O13 | 2.332(5) | Dy3-O3 | 2.369(4) | Dy5-O2 | 2.328(4) |
| Dy1-O19 | 2.309(5) | Dy3-O4 | 2.208(4) | Dy5-O25 | 2.364(4) |
| Dy1-N12 | 2.468(6) | Dy3-O16 | 2.389(4) | Dy5-O11 | 2.367(4) |
| Dy2-O25 | 2.386(4) | Dy3-O5 | 2.197(4) | Dy5-O20 | 2.332(4) |
| Dy2-O6 | 2.392(4) | Dy3-N7 | 2.491(5) | Dy5-O1 | 2.213(4) |

| | | | | | |
|---|---|---|---|---|---|
| Dy2-O7 | 2.426(4) | Dy3-N6 | 2.522(5) | Dy5-O10 | 2.407(4) |
| Dy2-O16 | 2.560(4) | Dy4-O2 | 2.314(4) | Dy5-O22 | 2.450(5) |
| Dy2-O23 | 2.354(4) | Dy4-O12 | 2.410(4) | Dy5-N1 | 2.512(5) |
| Dy2-O10 | 2.308(4) | Dy4-O25 | 2.429(4) | | |
| **Bond angles (°)** | | | | | |
| O8-Dy1-O18 | 103.4(2) | O25-Dy2-O6 | 98.81(13) | O2-Dy4-O12 | 97.78(14) |
| O8-Dy1-O17 | 82.73(19) | O12-Dy3-N7 | 87.54(15) | O2-Dy4-O25 | 69.92(13) |
| O8-Dy1-O13 | 82.0(2) | O12-Dy3-N6 | 127.81(15) | O2-Dy5-O25 | 70.84(14) |
| O8-Dy1-O19 | 92.52(19) | O6-Dy3-O12 | 72.12(13) | O2-Dy5-O11 | 72.44(14) |
| O8-Dy1-N12 | 72.9(2) | O6-Dy3-N7 | 64.54(15) | O2-Dy5-O20 | 75.97(16) |
| O7-Dy1-O18 | 76.01(16) | O6-Dy3-N6 | 143.93(15) | O2-Dy5-O10 | 132.12(14) |
| O7-Dy1-O17 | 123.62(17) | O3-Dy3-O12 | 64.38(13) | O2-Dy5-O22 | 146.45(16) |
| O25-Dy2-O6 | 98.81(13) | O3-Dy3-O6 | 122.25(13) | O2-Dy5-N1 | 62.84(15) |
| O25-Dy2-O7 | 79.66(14) | O2-Dy4-O12 | 97.78(14) | O25-Dy5-O11 | 79.27(13) |
| O25-Dy2-O16 | 74.45(13) | O2-Dy4-O25 | 69.92(13) | O25-Dy5-O10 | 69.68(13) |
| O25-Dy2-O15 | 72.76(13) | O2-Dy4-N3 | 62.85(14) | O25-Dy5-O22 | 102.23(17) |
| O25-Dy2-N9 | 140.75(14) | O2-Dy4-O21 | 82.57(15) | O25-Dy5-N1 | 131.17(14) |
| O25-Dy2-N10 | 125.36(15) | O2-Dy4-N4 | 125.72(15) | O11-Dy5-O10 | 74.56(15) |

**Table S5.** Selected bond lengths (Å) and angles (°) of **4**.

| **Bond lengths (Å)** | | | | | |
|---|---|---|---|---|---|
| Dy1-O12 | 2.350(5) | Dy2-O11 | 2.594(5) | Dy4-O2 | 2.330(4) |
| Dy1-O18 | 2.316(5) | Dy2-O12 | 2.701(5) | Dy4-O15 | 2.230(5) |
| Dy1-O7 | 2.414(5) | Dy2-O7 | 2.428(5) | Dy4-O9 | 2.435(5) |
| Dy1-O16 | 2.347(5) | Dy3-O11 | 2.383(5) | Dy4-O20 | 2.339(5) |
| Dy1-O13 | 2.431(5) | Dy3-O5 | 2.224(5) | Dy4-O19 | 2.398(5) |
| Dy1-O14 | 2.455(6) | Dy3-O2 | 2.357(5) | Dy5-O17 | 2.265(5) |
| Dy1-O8 | 2.194(5) | Dy3-O1 | 2.221(5) | Dy5-O19 | 2.407(5) |
| Dy1-N12 | 2.450(6) | Dy3-O9 | 2.488(5) | Dy5-O3 | 2.342(5) |
| Dy2-O11 | 2.594(5) | Dy3-O6 | 2.390(4) | Dy5-O4 | 2.196(5) |

| | | | | | |
|---|---|---|---|---|---|
| Dy2-O12 | 2.701(5) | Dy3-N7 | 2.462(6) | Dy5-O10 | 2.310(5) |
| Dy2-O7 | 2.428(5) | Dy3-N1 | 2.507(6) | Dy5-O21 | 2.273(5) |
| Dy2-O6 | 2.446(5) | Dy4-O2 | 2.330(4) | Dy5-N6 | 2.534(6) |
| Dy2-O22 | 2.351(5) | Dy4-O15 | 2.230(5) | | |
| Dy2-O19 | 2.396(4) | Dy4-O9 | 2.435(5) | | |
| **Bond angles (°)** | | | | | |
| O12-Dy1-O7 | 65.76(16) | O22-Dy2-O11 | 77.03(17) | O15-Dy4-O2 | 90.90(19) |
| O12-Dy1-O13 | 78.66(18) | O22-Dy2-O12 | 72.60(17) | O15-Dy4-O9 | 135.35(17) |
| O12-Dy1-O14 | 79.59(18) | O22-Dy2-O7 | 85.10(18) | O15-Dy4-O20 | 148.74(18) |
| O12-Dy1-N12 | 128.25(19) | O11-Dy3-N7 | 128.25(17) | O15-Dy4-O19 | 78.94(18) |
| O18-Dy1-O12 | 96.33(18) | O11-Dy3-N1 | 89.56(18) | O15-Dy4-O3 | 100.09(19) |
| O18-Dy1-O7 | 74.65(17) | O5-Dy3-O11 | 157.29(17) | O15-Dy4-N3 | 74.52(19) |
| O18-Dy1-O16 | 79.46(18) | O5-Dy3-O2 | 82.47(18) | O17-Dy5-O19 | 81.97(18) |
| O18-Dy1-O13 | 151.26(19) | O5-Dy3-O9 | 85.17(17) | O17-Dy5-O3 | 88.45(19) |
| O22-Dy2-O11 | 77.03(17) | O5-Dy3-O6 | 130.08(18) | O17-Dy5-O10 | 160.11(19) |
| O22-Dy2-O12 | 72.60(17) | O5-Dy3-N7 | 72.48(18) | O17-Dy5-O21 | 98.4(2) |
| O22-Dy2-O7 | 85.10(18) | O5-Dy3-N1 | 80.51(19) | O17-Dy5-N6 | 76.10(19) |
| O22-Dy2-O6 | 89.19(18) | O15-Dy4-O2 | 90.90(19) | O19-Dy5-N6 | 126.19(18) |
| O22-Dy2-O19 | 141.75(18) | O15-Dy4-O9 | 135.35(17) | O3-Dy5-O19 | 68.61(16) |

**Table S6.** Selected bond lengths (Å) and angles (°) of **5**.

| **Bond lengths (Å)** | | | |
|---|---|---|---|
| Dy1-O13 | 2.292(6) | Dy2-O8 | 2.162(5) |
| Dy1-O1 | 2.528(5) | Dy3-O7 | 2.164(5) |
| Dy1-O6 | 2.362(5) | Dy3-O6 | 2.359(5) |
| Dy1-O5 | 2.427(6) | Dy3-O9 | 2.418(12) |
| Dy1-O3 | 2.505(5) | Dy3-O3 | 2.390(5) |
| Dy1-O15 | 2.256(10) | Dy3-O4 | 2.626(9) |
| Dy1-O4 | 2.678(7) | Dy3-O11 | 2.483(9) |
| Dy1-N4 | 2.571(6) | Dy3-N2 | 2.512(7) |

| | | | |
|---|---|---|---|
| Dy1-N3 | 2.551(6) | Dy2-O1 | 2.380(5) |
| Dy2-O8 | 2.162(5) | Dy2-O5 | 2.408(5) |
| Dy2-O2 | 2.470(4) | Dy2-O12 | 2.369(6) |
| **Bond angles (°)** | | | |
| O1-Dy1-O4 | 120.2(2) | O8-Dy2-O1 | 133.23(18) |
| O1-Dy1-N4 | 62.11(18) | O8-Dy2-O5 | 146.6(2) |
| O1-Dy1-N3 | 123.71(18) | O8-Dy2-O12 | 86.8(2) |
| O6-Dy1-O1 | 161.39(18) | O8-Dy2-N6 | 71.34(19) |
| O6-Dy1-O5 | 111.73(19) | O2-Dy2-N6 | 117.12(18) |
| O6-Dy1-O3 | 63.69(17) | O7-Dy3-O9 | 83.3(3) |
| O6-Dy1-O4 | 63.9(2) | O7-Dy3-O3 | 151.2(2) |
| O6-Dy1-N4 | 126.16(19) | O7-Dy3-O4 | 135.8(2) |
| O6-Dy1-N3 | 63.32(19) | O7-Dy3-O11 | 77.0(3) |
| O8-Dy2-O1 | 133.23(18) | O7-Dy3-N2 | 73.0(2) |
| O8-Dy2-O5 | 146.6(2) | O6-Dy3-Dy1 | 34.33(13) |
| O8-Dy2-O12 | 86.8(2) | O6-Dy3-O9 | 106.6(3) |
| O8-Dy2-N6 | 71.34(19) | O6-Dy3-O3 | 65.54(18) |

## References.


[1] Sheldrick, G. M. *Acta Crystallogr., Sect. C: Struct. Chem*. **2015**, *71*, 3-8.

[2] Meng, T.; Liu, T.; Qin, Q. P.; Chen, Z. L.; Zou, H. H.; Wang, K.; Liang, F. P. Mitochondria-Localizing Dicarbohydrazide Ln Complexes and Their Mechanism of: In Vitro Anticancer Activity. *Dalton Trans.* **2020**, *49* (14), 4404–4415.

[3] Luo, Z.-R.; Wang, H.-L.; Zhu, Z.-H.; Liu, T.; Ma, X.-F.; Wang, H.-F.; Zou, H.-H; Liang, F.-P. Assembly of $Dy_{60}$ and $Dy_{30}$ Cage-Shaped Nanoclusters. *Commun. Chem.* 2020, **3(1)**, 30. https://doi.org/10.1038/s42004-020-0276-3.